INORGANIC SYNTHESIS AND INDUSTRIAL INORGANIC CHEMISTRY

Synthesis and Photocatalytic Properties of SiO$_2$–Cd$_2$SiO$_4$@CdS Nanocomposite Powders

A. A. Biryukov, E. Yu. Gotovtseva, and V. A. Svetlichnyi

Kuznetsov Siberian Physicotechnical Institute, National Research Tomsk State University,
pr. Lenina 36, Tomsk, 634050 Russia
e-mail: abba1983@mail.ru

Abstract—Inorganic composites SiO$_2$–Cd$_2$SiO$_4$@CdS were synthesized. The structure and morphology of the synthesized powders were studied. The composite materials obtained are more resistant to photocorrosion under both visible and UV radiation, compared to CdS particles deposited on SiO$_2$. The high photocatalytic activity of the synthesized SiO$_2$–Cd$_2$SiO$_4$@CdS composites was demonstrated by the example of photodegradation of Nile Blue dye in water under irradiation with visible light ($\lambda > 410$ nm).

Synthesis of photoactive materials successfully operating in a wide spectral range for decomposing organic pollutants in aqueous media and in air, and also, e.g., for generating hydrogen is a topical problem [1–6]. As a rule, photocatalysts based on titanium dioxide, which proved to be effective, are used for this purpose. "Pure" TiO$_2$ has a number of drawbacks: absorption only in the UV range ($\lambda < 380$ nm) and low quantum efficiency. Therefore, its additional sensitization is required. Photocatalysts based on nanoparticles of A^{II}B^{VI} semiconductors (CdS, CdZnS, etc.) [7–9] can be an alternative to TiO$_2$. Semiconductor nanoparticles of A^{II}B^{VI} group exhibit unique optical properties depending on their size, shape, and defectiveness [10, 11]. The difference in the spectral and luminescence properties of the same compound in the common and nanosized state is due to quantum size effects untypical of the given material in the macro state, which allows these nanoparticles to be used not only in medicine and biology as fluorescent markers, but also, as noted above, in photocatalysis for the decomposition of organic pollutants in water. However, fast recombination of electron–hole pairs, characteristic of A^{II}B^{VI} semiconductors, leads to low performance of catalysts based on them. Therefore, semiconductor particles, including those of CdS, are coated with a layer of a broader-band-gap semiconductor

or are doped with noble metals. Another problem arising when using nanoparticles of semiconductors, in particular, of CdS, as photocatalysts is their rapid oxidation or reduction [12] under the action of light (photocorrosion). Short illumination of powders or dispersions of CdS nanoparticles can lead to their deep photocorrosion with the formation of cadmium sulfate and sulfite (CdSO$_4$ and CdSO$_3$) or of elemental sulfur (CdS + $h^+ \rightarrow$ Cd^{2+} + S [13, 14]), which makes such particles unsuitable for use in photocatalytic processes. To prevent the photocorrosion, the particles are also coated or doped with other chemical elements or are embedded into inert matrices.

One of widely used inert supports for photoactive nanoparticles, including CdS, is silicon dioxide. Previously [15] we synthesized a composite material SiO$_2$/CdO/CdS, in which silicon dioxide was used as support. We found that introduction of cadmium ions in the step of the sol–gel synthesis of SiO$_2$, followed by the heat treatment, led to the formation of CdO and SiO$_2$ particles. Their subsequent impregnation in an H$_2$O/H$_2$S solution led to the formation of a complex structure with CdO, CdO@CdS, and CdS particles present in SiO$_2$. The mean radius of the formed CdS particles (or the CdS layer thickness) varied from 2.7 to 3.3 nm and depended on the size of the initial CdO particles. The photocatalytic

activity of the composites was studied by the examples of photodegradation of Nile Blue (NB) dye in alcohol and of hydrogen generation from an aqueous-methanol medium. In aqueous medium, these composites showed no photocatalytic activity because of efficient sorption of NB. These catalysts are also characterized by the photocorrosion of CdS particles, which led to poor stability of the photocatalyst.

This study was aimed at developing photocorrosion-resistant and photocatalytically active composite materials based on cadmium sulfide and on an inert silicon oxide matrix, efficiently operating in aqueous medium, and at studying the photocatalytic properties of the synthesized composites in both UV and visible ranges.

EXPERIMENTAL

The following chemicals were used for the synthesis: tetraethoxysilane (C$_2$H$_5$O)$_4$Si, Sigma–Aldrich, 99.7%; cadmium acetate (CH$_3$COO)$_2$Cd·2H$_2$O, Sigma–Aldrich, 99.5%; thioacetamide (TA), CH$_3$C(S)NH$_2$, Sigma–Aldrich, 99.0%; ethanol C$_2$H$_5$OH of LUX grade; ammonium hydroxide NH$_4$OH, 25%; and distilled water.

As a test object in studying the photocatalytic properties of the synthesized powders we used Nile Blue dye, C$_{20}$H$_{20}$ClN$_3$O$_5$, Aldrich, 95%.

Synthesis of inorganic photoactive SiO$_2$–Cd$_2$SiO$_4$@CdS powders. In a chemically resistant vessel, we mixed the following chemicals added in succession: (C$_2$H$_5$O)$_4$Si, C$_2$H$_5$OH, H$_2$O, and NH$_4$OH (volume ratio 1 : 1 : 0.5 : 0.075). The resulting mixture was stirred on a magnetic stirrer at 500 rpm for 90 min. After that, the vessel with the mixture was put on an electric hot plate, and the solvents (C$_2$H$_5$OH, H$_2$O) were evaporated to dryness to obtain a uniform powder of silicon dioxide SiO$_2$. The target product yield was no less than 95%, and the mean size of SiO$_2$ particles was about 400 nm (data of scanning electron microscopy, SEM).

Then, the powder was divided into several portions, and to each portion (m_{SiO_2} = 0.5 g) Cd(CH$_3$COO)$_2$·2H$_2$O was added in an amount of 0.006, 0.024, 0.083, 0.154, 0.308, or 0.64 g, so that the Cd : SiO$_2$ weight ratio in the samples was 0.5, 2.0, 7.0, 13.0, 26.0, and 54.0%, respectively. Then, the SiO$_2$–Cd(CH$_3$COO)$_2$ mixture was thoroughly ground in an agate mortar for 10 min. After that, it was placed in a muffle furnace and kept for 3 h at 900°C. The heat treatment resulted in the formation of

cadmium orthosilicate (data of X-ray diffraction analysis, XRD) along with SiO$_2$ as a result of direct sintering of cadmium with silicon dioxide.

Then, TA was dissolved separately in six vessels, each containing 10 mL of H$_2$O. The TA concentrations were chosen so as to ensure the cadmium and sulfur ratio in the samples Cd^{2+} : S^{2-} = 1 : 1. After that, annealed SiO$_2$–Cd$_2$SiO$_4$ powders were placed in these solutions. The resulting solutions were boiled for 2 min, after which they were cooled, water was decanted, and the resulting composites were washed with a large amount of H$_2$O to completely remove traces of organic products of TA decomposition.

The crystal structure of the powders was analyzed with an XRD 6000 X-ray diffractometer (Shimadzu, Japan; CuK$_\alpha$). A silicon powder was used as reference sample (a = 5.4309 Å). The diffraction patterns were scanned in the angle range 15°–45° with 0.03° step and accumulation time in each step of 1 s.

The surface morphology of the SiO$_2$–Cd$_2$SiO$_4$@CdS composites and the size characteristics were studied with a Quanta 200-3D scanning electron microscope (FEI, USA). The SiO$_2$–Cd$_2$SiO$_4$@CdS powders were preliminarily placed on a conducting adhesive tape to reduce the charge effect. The samples were examined in the following mode: beam current 5 μA, accelerating voltage 20 kV.

The pore structure parameters and the specific surface area were determined by the multipoint BET method using a TriStar II 3020 automatic gas adsorption analyzer (Micromeritics, USA). The specific surface area of the samples was determined from the low-temperature nitrogen adsorption. The powders were preliminarily degassed in a vacuum (10^{-2} mmHg) at 200°C for 2 h.

The absorption spectra of the synthesized powders were recorded on a Cary 100 spectrophotometer (Varian, Australia) equipped with a diffuse reflectance attachment (spectrum range 200–900 nm, resolution 1 nm). The samples (m = 0.02 g) were preliminarily ground with boric acid (m = 0.4 g) in an agate mortar.

The absorption spectra of aqueous NB solutions were recorded with an SM22 spectrophotometer (Solar, Belarus) in the range 250–750 nm. The optical path length was 1 cm.

The mean size of the CdS particles formed on the SiO$_2$–Cd$_2$SiO$_4$ surface was estimated from the absorption spectra using the semiempirical formula [16]

$$D = (-6.6521 \times 10^{-8})\lambda^3 + (1.9557 \times 10^{-4})\lambda^2$$
$$- (9.2352 \times 10^{-2})\lambda + 13.29,$$

where D is the particle size (nm), and λ is the position of the long-wave absorption band maximum (nm).

The photocatalytic activity of the synthesized SiO_2–Cd_2SiO_4@CdS powders was evaluated by the example of the NB photodegradation in water. Because the composites exhibit sorption properties, the NB solutions with the catalyst were allowed to stand for 24 h prior to irradiation. After that, their optical density was measured. The irradiation was performed under the following conditions. Glass test tubes, each containing 10 mL of aqueous NB solution ($c_{NB} = 10^{-5}$ M) and 8 mg of SiO_2–Cd_2SiO_4@CdS powders, were irradiated with a Sigma MD 2366 UV luminescent lamp (2×6 W) with the emission spectrum maximum at 365 nm or with a Philips Master CDM-TD 70W/942 broadband incandescent lamp (emission spectrum maximum 320–800 nm). In the case when the irradiation was performed with the incandescent lamp, ZhS-10 ($\lambda > 390$ nm) and ZhS-11 ($\lambda > 410$ nm) cutting color filters were additionally used. The irradiation was performed from below through a thin layer of the composite powder that underwent sedimentation on the test tube bottom. The distance between the lamps and solution being irradiated was 5 and 10 cm, respectively. In addition, to prevent heating of the medium, a fan was arranged from side of the end faces of the lamps under the samples being irradiated. After each irradiation run, the solutions were centrifuged for 5 min at a rate of 5000 rpm to remove the photocatalyst. The efficiency of the dye photodegradation was evaluated by a decrease in the optical density in the maximum of its long-wave absorption band ($\lambda = 634$ nm) relative to the decomposition of the dye irradiated under the same conditions without catalyst and with the same weighed portion of the commercial catalyst, titanium dioxide of Degussa P25 grade.

RESULTS AND DISCUSSION

As shown by X-ray diffraction, the heat treatment of the SiO_2–$Cd(CH_3COO)_2$ mixture at 900°C for 3 h leads to the formation of cadmium orthosilicate Cd_2SiO_4. The initial sample exhibits in the X-ray diffraction pattern only a broad band in the region of $2\theta \sim 22°$, belonging to amorphous silica. After the annealing (Fig. 1, curve 1), reflections with maxima at 18.9°, 23.6°, 30.1°, 32.1°, 33.5°, and 35.4°, belonging to Cd_2SiO_4 of rhombic structure (PDF no. 50527), and a weak reflection at 26.4°,

belonging to crystalline SiO_2 of hexagonal structure (PDF no. 9482), appear in the X-ray diffraction pattern.

Treatment of the SiO_2–Cd_2SiO_4 powders obtained with an aqueous thioacetamide solution leads to the appearance of a peak at 44.0° and to broadening and increase in the intensity of the reflection at 26.4° (Fig. 1, curve 2), suggesting the formation of CdS of hexagonal wurtzite-type structure (PDF no. 31075). Thus, cadmium sulfide is formed on the SiO_2–Cd_2SiO_4 surface. This also leads to a decrease in the intensity of the reflections belonging to SiO_2–Cd_2SiO_4.

The formation of cadmium sulfide is also proved by data of UV–visible absorption and Raman spectroscopy.

In the Raman spectra, there are broadened peaks with maxima in the regions of 300 and 600 cm^{-1}. The position of the peaks corresponds to cadmium sulfide of wurtzite structure [17], and the peak shifts and considerable broadening suggest small particle size and interaction of particles with the matrix.

In the absorption spectra of the composites, a characteristic edge of the exciton absorption band of cadmium sulfide also appears (Fig. 2). The edge of the CdS absorption band in the composites is in the range 480–620 nm. With an increase in the weight ratio of cadmium and TA relative to SiO_2, the optical density in the absorption spectra of the synthesized SiO_2–Cd_2SiO_4@CdS powders (Fig. 2) increases.

For the formed particles of CdS in SiO_2–Cd_2SiO_4, we calculated their mean size [16]. As follows from the calculations, in all the examined SiO_2–Cd_2SiO_4@CdS powders the mean size of the CdS particles or of their layer on the surface is 7 nm. On the other hand, according to the SEM data, the particle size of the SiO_2–Cd_2SiO_4@CdS composite as a whole is about 400 nm, and the particle shape is approximately spherical (Fig. 3).

For all the samples, the cadmium : precipitant (TA) ratio in the synthesis was 1 : 1. As noted above, the Cd_2SiO_4 phase is manifested in the X-ray diffraction patterns (Fig. 1, curve 2), though with lower intensity of reflections. Hence, the sulfidization in the course of treatment with TA is incomplete. It probably occurs only on the SiO_2–Cd_2SiO_4 surface.

According to the BET data, the specific surface area of the initially synthesized SiO_2–Cd_2SiO_4 samples is 3–4 m^2 g^{-1}, which is consistent with the submicrometer size of the particles (Fig. 3). As the cadmium concentration in the samples is increased, the specific surface area
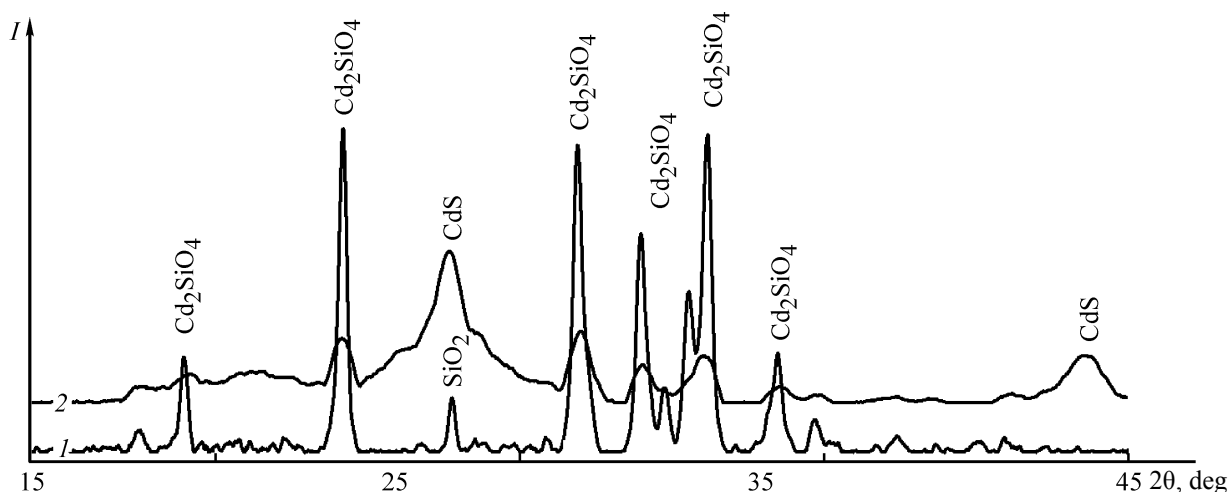
Fig. 1. Diffraction pattern of the (*1*) SiO$_2$–Cd$_2$SiO$_4$ powder (Cd content in SiO$_2$ 26 wt %) and (2) SiO$_2$–Cd$_2$SiO$_4$@CdS powder (Cd content in SiO$_2$ 26 wt %). (*I*) Intensity and (2θ) Bragg angle.

slightly decreases, which may be due to the formation of coarser particles. After the treatment of SiO$_2$–Cd$_2$SiO$_4$ with TA, the specific surface area of the samples starts to considerably decrease owing to the formation of a CdS layer on the particle surface. For example, the specific surface area of the sample with the initial Cd concentration of 7 and 13% after the treatment with TA becomes 1 and 0.5 m^2 g^{-1}, respectively. At higher Cd concentrations, the specific surface area of the samples decreases further and becomes undeterminable by the method used. A decrease in the specific surface area of the Cd$_2$SiO$_4$@CdS composites can be associated not only with an increase in the particle size as a result of formation of the CdS layer on the SiO$_2$–Cd$_2$SiO$_4$ surface, but also with plugging of open pores in the final material.

Photocatalytic activity of SiO$_2$–Cd$_2$SiO$_4$@CdS composites. The photodegradation of organic compounds under irradiation can occur as a result of intramolecular processes without additional agents, directly via interaction with electromagnetic radiation. However, introduction of photoactive particles (e.g., TiO$_2$, CdS, ZnO, etc.) into solutions favors acceleration of the photodegradation of organic molecules. In this case, semiconductor particles are direct participants of photocatalytic reactions. Under the action of radiation, free electrons and holes arise in the bulk of a semiconductor. Some of them migrate to the surface and are captured with it. Electrons can react with dissolved atmospheric oxygen to form strong oxidants, hydroxyl radicals and oxygen radical anions (•OH, •O$_2^-$), which efficiently oxidize organic compounds. In

turn, h^+ reacts with water or with any organic substance adsorbed on the catalyst surface [18]. As a result, organic pollutants decompose with the formation of products safe for humans [19].

A study of the sorption properties of SiO$_2$–Cd$_2$SiO$_4$@CdS composites by measuring the absorption spectra showed that approximately 30% of NB dye molecules were adsorbed from aqueous solutions ($V = 10$ mL, $c_{NB} = 1 \times 10^{-5}$ M) by 8-mg portions of all the composite samples. Figure 4, curve *2* shows the spectrum after the sorption by the catalyst with 54 wt % content of Cd in SiO$_2$.
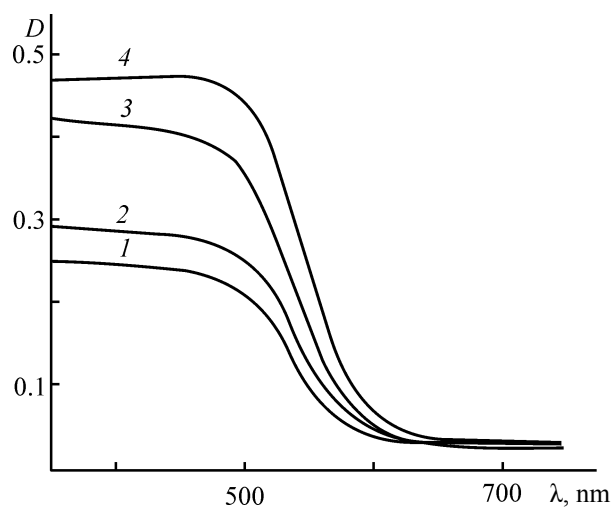
Fig. 2. Absorption spectra of SiO$_2$–Cd$_2$SiO$_4$@CdS powders. (*D*) Optical density and (λ) wavelength; the same for Fig. 4. Weight fraction of Cd in SiO$_2$, %: (*1*) 7, (*2*) 13, (*3*) 26, and (*4*) 54.
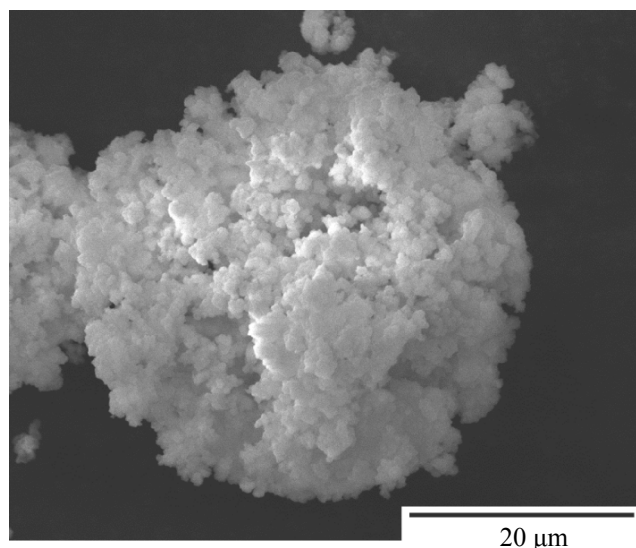
Fig. 3. SEM image of the surface of the SiO_2–Cd_2SiO_4@CdS powder, Cd weight fraction in SiO_2 26%.

Irradiation of NB solutions containing SiO_2–Cd_2SiO_4@CdS with both UV and visible light after the sorption leads to efficient decomposition of the dye, accompanied by a decrease in the optical density of the solution in the regions of both long-wave ($\lambda = 634$ nm) and short-wave ($\lambda = 278$ nm) absorption bands of NB. Figure 4 shows as example the absorption spectra of NB after the sorption (24 h) and irradiation with visible light
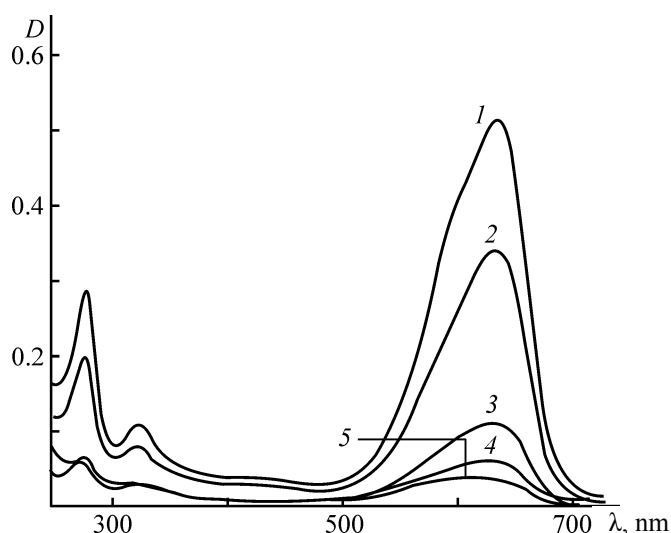
Fig. 4. Absorption spectra of NB in water. Spectra: (*1*) initial, (*2*) after 24-h sorption by the photocatalyst, and (*3–5*) after irradiation with an incandescent lamp ($\lambda > 390$ nm, ZhS-10 cutting color filter) in the presence of the photocatalyst for (*3*) 20, (*4*) 40, and (*5*) 60 min.

($\lambda > 390$ nm) in the presence of the catalyst containing 54 wt % Cd in SiO_2.

Figure 5 shows the kinetic curves of the NB photodegradation in aqueous solutions upon irradiation with different kinds of radiation in the presence of the SiO_2–Cd_2SiO_4@CdS catalyst and, for comparison, without catalyst and with the Degussa P25 TiO_2 photocatalyst.

Under UV irradiation with the luminescent lamp (365 nm), from 40 to 65% of the dye undergoes photodegradation in 60 min, and from 50 to 80%, in 2 h, depending on the concentration of cadmium introduced into SiO_2 (Fig. 5a). Without catalyst, about 9% of NB decomposes in 2 h. The commercial titanium dioxide powder (Degussa P25) exhibits the highest performance: Approximately 98% of the dye decomposes in its presence in 40 min. The decomposition of the dye on TiO_2 in the UV range is due to high absorbance of titanium dioxide in this range and to high efficiency of photocatalysis. The synthesized SiO_2–Cd_2SiO_4@CdS composites show lower performance in the UV range compared to TiO_2. This is caused by a number of factors, in particular, by the lower absorbance of cadmium sulfide in the region of 365 nm compared to TiO_2 and by the lower area of the interaction (the specific surface area of Degussa P25 TiO_2 is about 50 m^2 g^{-1}, whereas that of SiO_2–Cd_2SiO_4@CdS is as low as 1 m^2 g^{-1}).

The results of studying the kinetics of the NB photodegradation under illumination with the broadband visible radiation of the incandescent lamp are shown in Figs. 5b and 5c. Without photocatalyst, the degree of NB decomposition in 60 min was about 18%. In the presence of Degussa P25 TiO_2 photocatalyst, the degree of NB decomposition after irradiation for 1 h (Figs. 5b, 5c, curves *2*) was about 86% at $\lambda > 390$ nm (ZhS-10) and about 80% at $\lambda > 410$ nm (ZhS-11). In the presence of the SiO_2–Cd_2SiO_4@CdS composite, from 78 to 93% of NB dye undergoes photodegradation upon irradiation with visible light for 1 h, depending on the CdS concentration (Figs. 5b, 5c, curves *3–6*).

Thus, in contrast to UV irradiation, under irradiation with visible light the efficiency of the decolorization of the NB solution in the presence of the SiO_2–Cd_2SiO_4@CdS composite is comparable with that reached in the presence of Degussa P25 TiO_2 photocatalyst, and at high CdS concentrations (26 and 54%) it is even higher. Furthermore, as we found, in the case of photocatalysis in the presence of TiO_2 with visible light irradiation the major process is the dye photosorption on TiO_2,
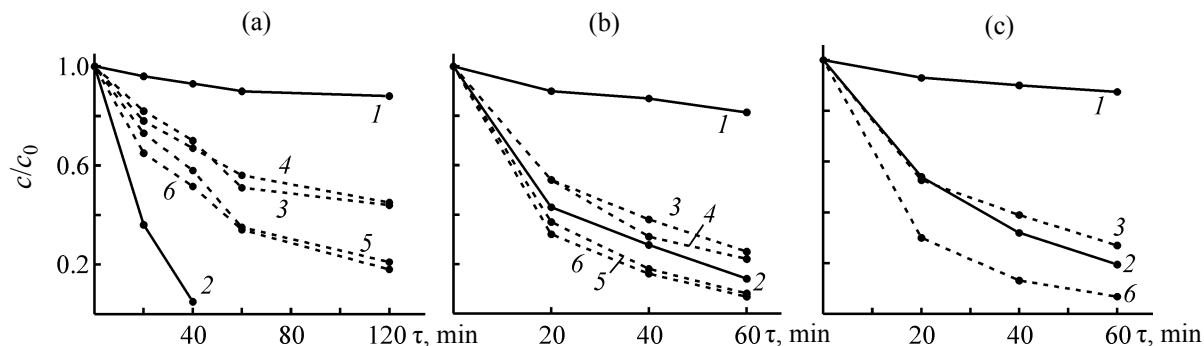
Fig. 5. Photodegradation of NB in aqueous solution upon (a) UV irradiation and (b, c) irradiation with an incandescent lamp with (b) ZhS-10 ($\lambda > 390$ nm) and (c) ZhS-11 ($\lambda > 410$ nm) cutting filters. (c/c_0) Relative concentration and (τ) irradiation time. (*1*) Without catalyst, (*2*) with commercial Degussa P25 TiO$_2$ catalyst, and (*3–6*) with SiO$_2$–Cd$_2$SiO$_4$@CdS. Cd content in SiO$_2$, wt %: (*3*) 7, (*4*) 13, (*5*) 26, and (*6*) 54.

manifested in coloration of titanium dioxide particles, rather than the dye photodegradation. Further prolonged irradiation (>4 h) of these solutions containing TiO$_2$ with visible light does not lead to the decolorization of the dye sorbed on the particles. In the case of the SiO$_2$–Cd$_2$SiO$_4$@CdS composites, the dye molecules sorbed on the particle surface are decolorized also. In 90–120 min (depending on the CdS concentration in the composite), the solutions are completely decolorized, and the initial yellow color of the composite is restored.

To determine the photostability and operation life of the synthesized composites, we performed cyclic studies of their photocatalytic activity (Fig. 6). The initial concentration of the dye in the solution was 10^{-4} M (10 times higher than in the previous experiment). One irradiation cycle lasted for 4 h, after which the solution

was centrifuged, and its optical density was measured. Then, an aqueous NB solution ($c_{NB} = 10^{-4}$ M) was added to the SiO$_2$–Cd$_2$SiO$_4$@CdS powder separated by centrifugation, and the irradiation was repeated. As seen from Fig. 6, after the first 4-h irradiation cycle, the residual concentration of NB dye in the solution is about 7%; after the second cycle, it is 10%, and after the third cycle, 21%. Further irradiation of the latter solution for 8 h leads to its complete decolorization. Certain residual amount of the dye remains on the SiO$_2$–Cd$_2$SiO$_4$@CdS composites, which also suggests additional photoinduced sorption of the dye molecules on the catalyst surface. Experiments on irradiation of Nile Blue solutions under similar conditions with commercial titanium dioxide showed that the residual NB content in water after 4-h irradiation was 92%, and further irradiation did not lead
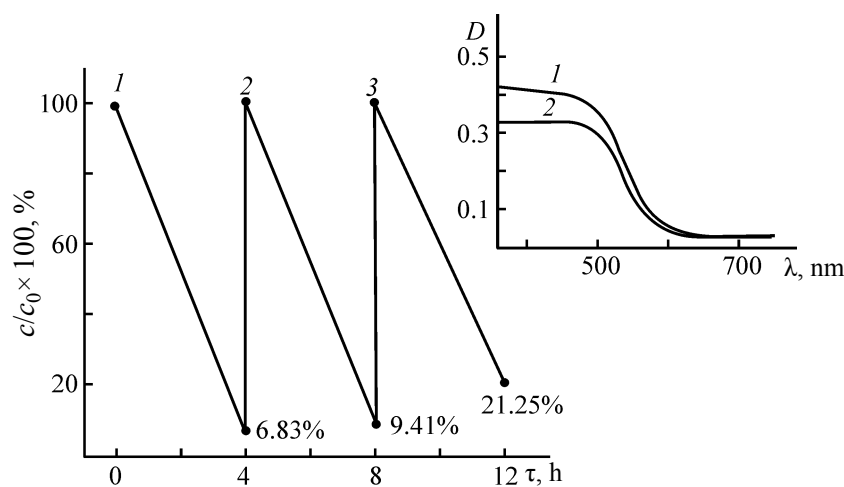
Fig. 6. Variation of the NB concentration in solutions, c/c_0, in repeated irradiation runs with an incandescent lamp with ZhS-11 cutting filter ($\lambda > 410$ nm) in the presence of the SiO$_2$–Cd$_2$SiO$_4$@CdS composite, weight fraction of Cd in SiO$_2$ 26%. Insert: absorption spectra of this composite (*1*) before irradiation and (*2*) after irradiation for 12 h. (*D*) Optical density, (λ) wavelength, and (τ) irradiation time.

to the NB decomposition. Thus, as noted above, visible irradiation in the presence of titanium dioxide does not lead to the photodegradation of NB dye, and only efficient photoinduced sorption of the dye molecules on the surface of catalyst particles is observed.

Analysis of the absorption spectra of the SiO_2–Cd_2SiO_4@CdS composite specially irradiated for 12 h in aqueous solution without the dye shows that the changes caused by the photocorrosion amount to approximately 20% (Fig. 6, insert). Experiments on irradiation under similar conditions of the previously synthesized composites SiO_2/CdO/CdS [15], performed for comparison, showed that these composites underwent considerable decolorization (by more than an order of magnitude).

CONCLUSIONS

(1) The SiO_2–Cd_2SiO_4@CdS composite was synthesized in three steps. In the first step, submicrometer SiO_2 powder was prepared by the sol–gel method. In the second step, crystalline composite of silicon dioxide with cadmium orthosilicate was prepared by sintering of SiO_2 with cadmium acetate. In the third step, an approximately 7 nm thick layer of cadmium sulfide was formed on the surface of SiO_2–Cd_2SiO_4 particles to obtain the SiO_2–Cd_2SiO_4@CdS composite material.

(2) Studies of Nile Blue photolysis in the presence of SiO_2–Cd_2SiO_4@CdS showed that this composite exhibits photocatalytic properties. It exhibits higher photostability than separate CdS particles or CdS particles deposited on the surface of the SiO_2 support do, as it is less susceptible to photocorrosion. Owing to longer-wave absorption, compared to the known commercial catalyst, Degussa P25 TiO_2, the composite we prepared shows higher performance in photocatalysis under visible radiation.

ACKNOWLEDGMENTS

REFERENCES

1. Zhao, W., Ma, W., Cher, C., et al., *J. Am. Chem. Soc.*, 2004, vol. 126, pp. 4782–4783.

2. Yang, Y., Wu, Q., Guo, Y., et al., *J. Mol. Catal. A: Chemical*, 2005, vol. 225, pp. 203–212.

3. Chen, C., Ma, W., and Zhao, J., *Chem. Soc. Rev.*, 2010, vol. 39, pp. 4206–4219.

4. Zhao, D., Chen, C., Wang, Y., et al., *Environ. Sci. Technol.*, 2008, vol. 42, pp. 308–314.

5. Ma, W., Li, J., Tao, X., et al., *Angew. Chem.*, 2003, vol. 115, pp. 1059–1062.

6. Ran, J., Yu, J., and Jaroniec, M., *Green Chem.*, 2011, vol. 13, pp. 2708–2713.

7. Zhua, H., Jianga, R., Xiao, L., et al., *J. Hazard. Mater.*, 2009, vol. 169, pp. 933–940.

8. Ma, H., Yan, H., Shi, J., et al., *J. Catal.*, 2008, vol. 260, pp. 134–140.

9. Wang, L., Wang, W., Shang, M., et al., *Int. J. Hydrogen Energy*, 2010, vol. 35, pp. 19–25.

10. Lakowicz, J.R., Gryczynski, I., et al., *J. Phys. Chem.* B, 1999, vol. 103, pp. 7613–7620.

11. El-Sayed, M.A., *Acc. Chem. Res.*, 2004, vol. 37, pp. 326–333.

12. Wu, W., Liu, G., Xie, Q., et al., *Green Chem.*, 2012, vol. 14, pp. 1705–1709.

13. Meissner, D., Memming, R., and Kastening, B., *J. Phys. Chem.*, 1988, vol. 92, pp. 3476–3483.

14. Frank, A.J. and Honda, K., *J. Phys. Chem.*, 1982, vol. 86, pp. 1933–1935.

15. Biryukov, A.A., Gotovtseva, E.Yu., Svetlichnyi, V.A., et al., *Russ. J. Appl. Chem.*, 2014, vol. 87, pp. 1599–1606.

16. Yu, W.W., Qu, L., Guo, W., et al., *Chem. Mater.*, 2003, vol. 15, pp. 2854–2860.

17. Singh, V. and Chauhan, P., *Chalcogen. Lett.*, 2009, vol. 6, pp. 421–426.

18. Zhao, J., Chen, C., and Ma, W., *Topics Catal.,* 2005, vol. 35, pp. 269–278.

19. Pang, Y.L., Abdullah, A.Z., and Bhatia, S., *Desalination*, 2011, vol. 277, pp. 1–14.